ISSN 0036-0244, Russian Journal of Physical Chemistry A, 2015, Vol. 89, No. 11, pp. 2032–2035. © Pleiades Publishing, Ltd., 2015.
Original Russian Text © V.O. Kazak, P.A. Chernavskii, G.V. Pankina, A.Y. Khodakov, V.V. Ordomsky, 2015, published in Zhurnal Fizicheskoi Khimii, 2015, Vol. 89, No. 11, pp. 1768–1772.

DEDICATED TO THE JOURNAL'S 85th ANNIVERSARY

Effect of a Carrier's Nature on the Activation of Iron-Supported Catalysts[1]

V. O. Kazak[a], P. A. Chernavskii[a], G. V. Pankina[a], A. Y. Khodakov[b], and V. V. Ordomsky[b]

[a] *Faculty of Chemistry, Moscow State University, Moscow, 119991 Russia*
[b] *Unité de Catalyse et de Chimie du Solide, Université Lille1 Cité Scientifique, 59655 Villeneuve d'Ascq cedex, France*
e-mail: vladislavkazak@gmail.com

Received February 2, 2015

Abstract—The effect a carrier's nature has on the activation of iron-supported catalysts in a stream of pure carbon monoxide CO is investigated. It is shown that iron is mainly found in the form of magnetite Fe_3O_4 for carbon supports and in the form of hematite Fe_2O_3 for silica gel supports. It is shown that all activated samples are chiefly made up of the Hägg carbide χ-Fe_5C_2, but its concentration is higher for the carbon supports.

Keywords: iron oxide nanoparticles, catalyst, carbides, Fischer–Tropsch synthesis.

DOI: 10.1134/S0036024415110060

INTRODUCTION

In recent decades, growing numbers of researchers have become interested in Fischer–Tropsch synthesis (FTS) as an alternative method for the industrial production of a variety of chemicals, from alkanes to oxygenates [1, 2]. Iron is often used as an active component of FTS catalyst [3]. Most of the experimental data obtained so far indicate that the active phase of iron FTS catalyst is made up of different iron carbides [4–6]. These catalysts must therefore be activated before performing catalytic investigations.

It is known [5] that iron catalysts can be activated by pure hydrogen, pure carbon monoxide, or a mixture of the two. It is also known that activation by pure carbon monoxide results in the best catalytic behavior [7]. It has been established that both the activity and selectivity of FTS catalyst depend on the composition of the gas used for activation. In [8], however, Bartholomew et al. showed that the nature of the activating gas affected the activity of the catalyst only over 100 h of catalytic tests. Earlier investigations of the activation of iron catalysts were chiefly performed on catalyst synthesized using only one support. The effect the nature of the support had on the activation of iron catalyst was not studied.

In this work, we studied the activation of monometallic iron-supported catalysts and the effect the nature of the carrier had on this process.

EXPERIMENTAL

Catalyst Preparation

All catalysts were synthesized via conventional incipient wetness impregnation (iron weight content, 10 wt %). As supports, we used silica gel (CARiACT Q-10, Fuji Silysia); SBA-15 prepared by method described in [9]; multiwalled carbon nanotubes (CNT; purity ⩾ 95%; external diameter, 20–30 nm; Chengdu Organic Chemistry); and ordered mesoporous carbon CMK-3, prepared by the method described in [10]. Prior to use, the multiwalled carbon nanotubes were activated via refluxion in concentrated (65 wt %) nitric acid at 120°C over 16 h. After impregnation, all samples were dried at 100°C for 24 h and then calcined at 400°C for 6 h in an air (Fe/SiO_2 and Fe/SBA-15) or nitrogen (Fe/CNT and Fe/CMK-3) flow.

Nitrogen Physisorption

The BET surface area, pore volume, and average pore diameter were determined via N_2 physisorption using an automated Micromeritics ASAP 2000 system. The samples were degassed under vacuum at <10 mm Hg at 300°C for 4 h prior to N_2 physisorption.

X-Ray Powder Diffraction

Ex situ X-ray powder diffraction (XRD) experiments were conducted using a Bruker AXS D8 diffractometer (Cu*K*α radiation, nickel monochromator). The XRD patterns were collected in the 20–70° (2θ) range. The average crystallite size of Fe_3O_4, Fe_2O_3, or

---

[1] This article was translated by the authors.

Table 1. Textural properties of the investigated samples

Sample	Surface area S_{BET}, m^2/g	Pore volume V_{total}, cm^3/g	Average pore diameter $d_{avr.}$, nm
Fe/SiO$_2$	307	1.31	17.5
Fe/SBA-15	1045	1.39	7.7
Fe/CNT	163	0.56	5.0
Fe/CMK-3	1326	1.32	3.8

iron carbides was calculated from the most intense diffraction peaks, according to the Scherrer equation [11].

Magnitometric Investigation

The activation process was studied magnitometrically *in situ* [12] in the thermoprogrammed mode in a flow of pure carbon monoxide (GHSV 64000 h^{-1}). All samples were heated to 200°C with 6.6°C/min ramping, held for 10 min, and then sequentially heated to 350°C with 4.7°C/min ramping and held for 120 min. After activation, each sample was cooled to room temperature in a flow of CO. During treatment, the saturation magnetization curve was recorded by a magnetometer in a magnetic field of 0.3 T.

RESULTS AND DISCUSSION

Data on the textural properties of samples prepared using different supports are presented in Table 1. The characteristics of the selected supports varied widely. SiO$_2$ has mostly large mesopores formed by the volume between globules with surface areas of ~300 m^2/g. SBA-15 consists of hexagonal cylindrical pores, connected to one another by small micropores in their walls with surface areas of ~1000 m^2/g; this is consistent with the data in [9]. The structural properties of CMK-3 were in good agreement with those of SBA-15, on whose basis our carrier was obtained.

The textural properties of CMK-3 were created by filling the mesopores of an SBA-15 template with sucrose with subsequent removal of the template. CMK-3 is thus formed by interconnected carbon rods and has a surface very similar to that of SBA-15. The size of the CMK-3 pores is smaller (3.8 nm) than that of SBA-15 due to the thinness of the SBA-15 walls, relative to the diameter of the mesopores. The nanotubes of the CNT have uniform diameters of about 5 nm. The relatively high surface area indicates that the nanotubes have open caps.

X-ray patterns obtained for catalysts calcined and activated in CO are shown in Fig. 1. The spectra are distinguished by iron-containing phases (Fe$_3$O$_4$, Fe$_2$O$_3$, χ-Fe$_5$C$_2$) observed at different stages of catalyst preparation. These patterns show that phase composition of calcined samples depended largely on the nature of the support. Magnetite Fe$_3$O$_4$ is the mainly iron-containing phase for carbon supported catalysts while hematite Fe$_2$O$_3$ is the one for those based on silica gel. The phase composition of activated catalysts does not depend on the nature of the support, and

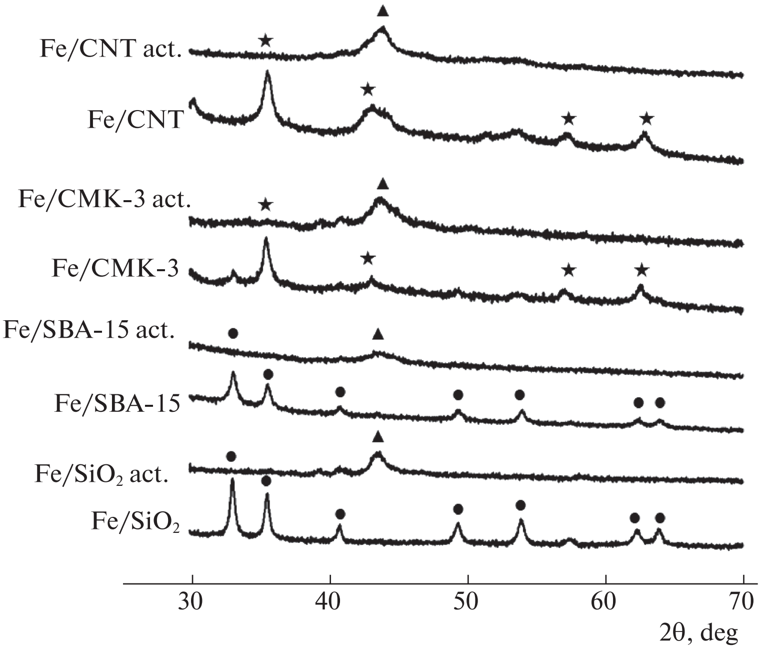

Fig. 1. XRD patterns of calcined and activated samples on (a) silica gel and (b) carbon supports: ★, Fe$_3$O$_4$; •, Fe$_2$O$_3$; and ▲, χ-Fe$_5$C$_2$, respectively.

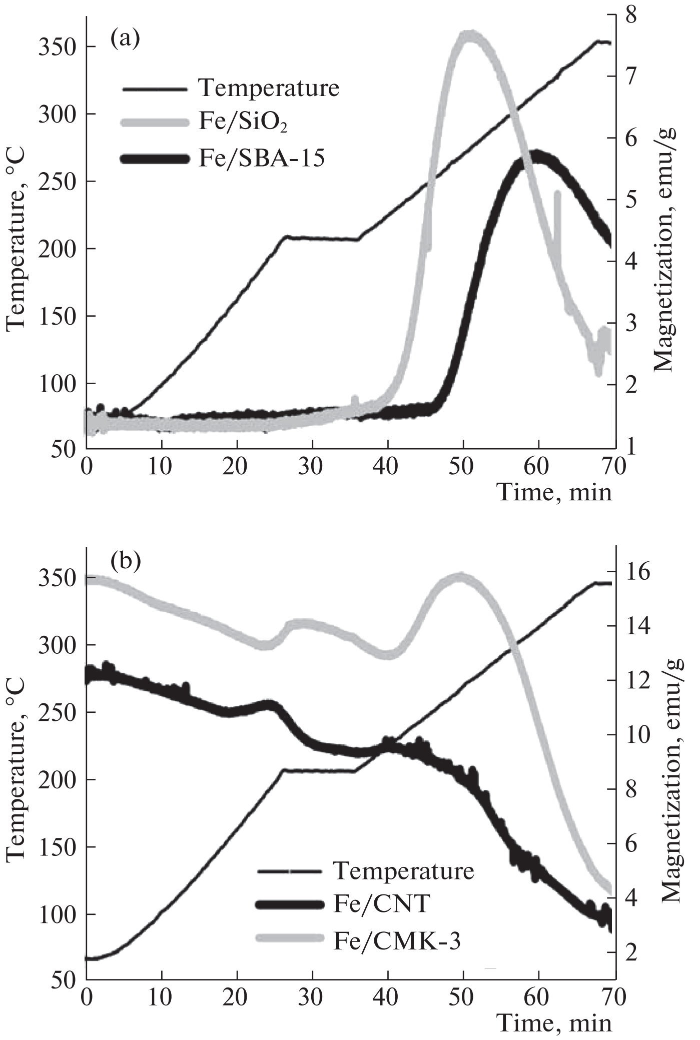

Fig. 2. Sample magnetization after thermo-programmed activation in CO: (a) Fe/SiO_2 and Fe/SBA-15; (b) Fe/CNT and Fe/CMK-3.

their mainly iron containing phase is Hägg-carbide χ-Fe_5C_2.

The XRD data are consistent with the magnitometric results from activation in a CO flow (Figs. 2–3, Table 2). The initial values of magnetization for samples prepared using carbon supports is higher than those for silica samples. The considerable difference between the initial magnetization values for different supports confirms that ferrimagnetic magnetite Fe_3O_4 is the mainly iron-containing phase for carbon supported catalysts while antiferromagnetic hematite Fe_2O_3 is the one for those based on silica gel. It would seem that magnetite forms during calcination in a nitrogen flow due to the reaction between iron oxide and the carbon of a support.

The increased magnetization at ~150°C and 250°C for Fe/CNT and Fe/CMK-3, respectively, resulted from the formation of additional amounts of magnetite in CO flows. Subsequent heating reduced the magnetization, due possibly to the formation of Hägg carbide χ-Fe_5C_2, which has a lower Curie temperature (~256°C). In contrast, Fe/SiO_2 and Fe/SBA-15 catalysts have no initial magnetization, and an increase in magnetization is observed only at temperatures higher than 200°C. The maximum values of magnetization were observed at 270°C and 300°C for Fe/SiO_2 and Fe/SBA-15, respectively.

The crystallite sizes of nanoparticles in the catalysts before and after activation were estimated using the Scherrer equation (Table 2). Except for Fe/CNT catalyst, our values of the average sizes correspond to those of the average pore diameter. We may assume that most of the particles are located in the support's pores for the Fe/SiO_2, Fe/SBA-15, and Fe/CMK-3 samples, and on surfaces of carbon nanotubes for Fe/CNT. In addition, the average crystallite sizes fall several times for all samples after activation. This can be explained by a drop in crystallinity during thermo-

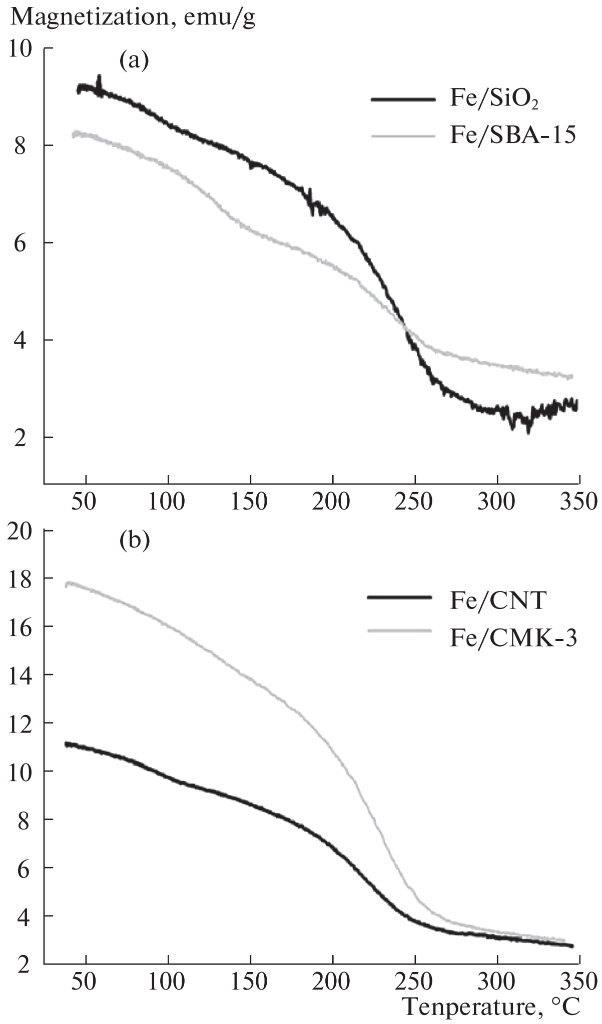

Fig. 3. Thermomagnetic curves of activated catalyst: (a) Fe/SiO_2 and Fe/SBA-15; (b) Fe/CNT and Fe/CMK-3.

programmed activation in a CO flow. It should be noted that our data shows particle size depends on the nature of the support.

Thermomagnetic curves were obtained to determine the qualitative composition of the activated catalysts (Fig. 3). The figure shows a considerable increase in magnetization for most of the catalysts when the temperature falls below 250°C, indicating χ-Fe_5C_2 was present in these samples. In addition, the increased magnetization of the carbon-supported catalyst is higher than that of ones based on silica when cooled to room temperature. This suggests that the concentration of Hägg-carbide χ-Fe_5C_2 is greater for carbon-supported catalysts, since we know that magnetization is directly proportional to mass. However, the magnetization for all samples was not zero at 350°C, due probably due to small amounts of phase that had higher Curie temperature (e.g., magnetite). However, the XRD results do not confirm this assumption, perhaps because of the small size of the particles.

Table 2. XRD and magnetometric results

Sample	After calcination		After activation in CO	
	Average particle size, nm	Magnetization at $T = 300$ K, emu/g	Average particle size, nm	Magnetization at $T = 300$ K, emu/g
Fe/SiO_2	17.5	0.1	6.1	9.2
Fe/SBA-15	9.4	0.2	2.0	8.3
Fe/CNT	12.3	12.5	4.1	11.1
Fe/CMK-3	3.8	12.6	1.8	18.2

CONCLUSIONS

Iron is mainly present in the form of magnetite Fe_3O_4 in carbon supports and in the form of hematite Fe_2O_3 in ones based on silica gel. It was established that all activated samples were chiefly made up of the Hägg carbide χ-Fe_5C_2, but its concentration was higher for the carbon supports.

REFERENCES

1. E. Iglesia, S. L. Soled, and R. A. Fiato, J. Catal. **137**, 212 (1992).
2. A. Y. Khodakov, W. Chu, and P. Fongarland, Chem. Rev. **107**, 1692 (2007).
3. S. Li, S. Krishnamoorthy, A. Li, et al., J. Catal. **206**, 202 (2002).
4. M. E. Dry, Stud. Surf. Sci. Catal. **152**, 533 (2004).
5. J. W. Niemantsverdriet, A. M. van der Kraan, W. L. van Dijk, et al., J. Phys. Chem. **84**, 3363 (1980).
6. M. D. Shroff, D. S. Kalakkad, K. E. Coulter, et al., J. Catal. **156**, 185 (1995).
7. M. Luo, H. Hamdeh, and B. H. Davis, Catal. Today **140**, 127 (2009).
8. J. Xu and C. H. Bartholomew, J. Phys. Chem. B **109**, 2392 (2005).
9. A. Y. Khodakov, A. Griboval-Constant, R. Bechara, et al., J. Catal. **206**, 230 (2002).
10. S. Jun, S. H. Joo, R. Ryoo, et al., J. Am. Chem. Soc. **122**, 10712 (2000).
11. P. Scherrer, Göttinger Nachricht. Gesell. **2**, 98 (1918).
12. P. A. Chernavskii, B. S. Lunin, R. A. Zakharyan, et al., Instrum. Exp. Tech **57**, 78 (2014).